Journal of Autoimmunity 100 (2019) 40–51

Contents lists available at ScienceDirect

Journal of Autoimmunity

journal homepage: www.elsevier.com/locate/jautimm

Endogenous double-stranded Alu RNA elements stimulate IFN-responses in relapsing remitting multiple sclerosis

Maxwell J. Heinrich[a], Caroline A. Purcell[a], Andrea J. Pruijssers[b], Yang Zhao[c], Charles F. Spurlock III[a], Subramaniam Sriram[d], Kristen M. Ogden[b], Terence S. Dermody[e], Matthew B. Scholz[f], Philip S. Crooke III[g], John Karijolich[c], Thomas M. Aune[a,c,*]

[a] Departments of Medicine, Vanderbilt University Medical Center, Nashville, TN 37212, USA
[b] Departments of Pediatrics, Vanderbilt University Medical Center, Nashville, TN 37212, USA
[c] Departments of Pathology, Microbiology and Immunology, Vanderbilt University Medical Center, Nashville, TN 37212, USA
[d] Departments of Neurology, Vanderbilt University Medical Center, Nashville, TN, 37212, USA
[e] Departments of Pediatrics and of Microbiology and Molecular Genetics, University of Pittsburgh School of Medicine, Pittsburgh, PA, USA
[f] Vanderbilt Technologies for Advanced Genomics, Vanderbilt University Medical Center, Nashville, TN, 37212, USA
[g] Department of Mathematics, Vanderbilt University, Nashville, TN, 37212, USA

ARTICLE INFO

Keywords:
Relapsing remitting multiple sclerosis
Double stranded RNA sensor
Interferons
Alu retrotransposon

ABSTRACT

Various sensors that detect double-stranded RNA, presumably of viral origin, exist in eukaryotic cells and induce IFN-responses. Ongoing IFN-responses have also been documented in a variety of human autoimmune diseases including relapsing-remitting multiple sclerosis (RRMS) but their origins remain obscure. We find increased IFN-responses in leukocytes in relapsing-remitting multiple sclerosis at distinct stages of disease. Moreover, endogenous RNAs isolated from blood cells of these same patients recapitulate this IFN-response if transfected into naïve cells. These endogenous RNAs are double-stranded RNAs, contain Alu and Line elements and are transcribed from leukocyte transcriptional enhancers. Thus, transcribed endogenous retrotransposon elements can co-opt pattern recognition sensors to induce IFN-responses in RRMS.

1. Introduction

Multicellular organisms contain an array of pattern recognition systems that serve as a first line of defense against both bacterial and viral infections [1–6]. Examples include the toll-like receptors (TLR), C-type lectin receptors (CLR), NOD-like receptors (NLR), and DExD/H-box helicases such as RIG-I and MDA5. While RIG-I and MDA5 are expressed by most cell lineages, TLR3 exhibits a more restricted expression pattern. Differences in dsRNA recognition also exist among these sensors, with RIG-I recognizing short (< 400 nucleotides) 5' triphosphate uncapped dsRNA or ssRNA and MDA5 recognizing dsRNA that is over 2000 nucleotides. Both TLR3 and the DExD/H-box helicases, RIG-I and MDA5, induce IFNs that may vary depending upon cell type in response to stimulation by viral double-stranded RNA (dsRNA). IFN classes include type 1 IFNs, IFN-α and IFN-β, type 2 IFN, IFN-γ, and type 3 IFN, IFN-λ (also named IL-29, IL28A and IL28B, respectively) [7–12]. Type 1 and type 2 IFNs exhibit potent antiviral effects by inducing similar but not entirely overlapping sets of genes with antiviral properties. IFN-γ is also a critical macrophage-activating factor and plays a key role in cell-mediated immunity. The type 1 interferons (IFN), e.g. IFN-α, IFN-β, also play important roles in innate immune responses. IFNs, via class-specific IFN cell surface receptors activate transcription factors termed IFN regulatory factors (IRFs) that bind to conserved DNA enhancer elements termed IFN-stimulated response elements (ISREs) resulting in induction of 100s of IFN-responsive genes [13].

Through a variety of mechanisms, including induction of these IFN-responsive genes, IFNs induce antiviral responses, which may culminate in death of virus-infected cells and neighboring cells to control viral infection. Pathogen-associated molecular patterns, such as dsRNA, and cellular damage-associated molecular patterns can also prime the NLR sensor molecule NLRP3 to oligomerize into inflammasomes. This priming often occurs in association with activation of other innate sensor molecules, such as TLR3. Inflammasomes activate the caspase-1 cascade, which leads to production of pro-inflammatory cytokines, including IL-1β and IL-18, and cell death.

IFN-responses have been documented in the absence of an obvious source of bacterial or viral infection. Such responses have been

* Corresponding author. Departments of Medicine, Vanderbilt University Medical Center, Nashville, TN 37212, USA.
E-mail address: tom.aune@vanderbilt.edu (T.M. Aune).

https://doi.org/10.1016/j.jaut.2019.02.003
Received 28 November 2018; Received in revised form 15 February 2019; Accepted 20 February 2019
Available online 28 February 2019
0896-8411/

observed in the setting of human autoimmune disease, most notably systemic lupus erythematosus [14], and to a lesser extent relapsing remitting multiple sclerosis (RRMS), rheumatoid arthritis (RA), Sjogren's disease (Sj) and others, as well as certain cancers [15–24]. In these human conditions, sources of stimuli leading to induction of IFNs are not entirely clear. The extent to which these same pattern recognition sensors described above can be co-opted by the host in the absence of pathogen infection to induce a kind of sterile IFN-response is incompletely understood. Various eukaryotic RNAs form stem-loop structures, in which the stem is a dsRNA structure and the loop is single stranded RNA, as part of their natural biology. These RNAs do not routinely activate innate cellular dsRNA sensing pathways and induce IFNs. However, mis-processing of these RNAs may produce an imbalance in their dsRNA character or their cellular location leading to activation of innate dsRNA sensors [25–28].

Additional sources of dsRNA structures that exist in mammalian cells are RNAs produced by the retrotransposon class of genetic elements [26,29–31]. Two sub-classes of these elements are the long-interspersed element (LINE, up to ~6000 bp in length) and the short-interspersed element (SINE, ~300 bp in length) and have sequence similarity to retroviruses. Alu elements are SINE elements unique to primates. About 1,000,000 LINE elements and 1,000,000 Alu elements exist in human genomes. As part of their normal life cycle, LINE and Alu elements can be transcribed into RNAs, converted to DNA by endogenous reverse transcriptase and reintegrated into unique sites in the genome. Insertion of these retrotransposons into critical sites in the genome, such as protein-coding exons or 3′ untranslated regions can be deleterious to the host and, in fact, has been linked to human disease. Other sources of LINE and Alu RNAs that may exist within cells include those transcribed as part of exons, introns, 3' untranslated regions of protein coding genes and those transcribed as part of enhancer RNAs (eRNAs). Considering the general view that 70–80% of the human genome is transcribed by some cell during some stage of development, it seems likely that LINE and Alu RNAs may make a significant contribution to the total amount of RNA present in a given eukaryotic cell. Importantly, both Alu and LINE RNAs bind to dsRNA pattern recognition sensors indicating they possess a dsRNA structure [20,26,32]. Thus, alterations in transcription or degradation of Alu and LINE RNAs, either as unique elements as part of their normal life cycle or as part of another RNA species, e.g. pre-mRNA, mRNA, eRNA, may alter activation of dsRNA sensors and corresponding cellular phenotypes.

Extensive mis-processing of RNAs, including rRNAs, Y RNAs, U snRNAs, and exon loss and intron retention of mRNAs, is found in leukocytes isolated from RRMS patients [33]. Therefore, the purpose of studies performed here was to identify RRMS patients with elevated leukocyte IFN-responses, determine if RNA isolated from these RRMS leukocytes could recapitulate these IFN-responses when transfected into naïve cells and determine the identity of these RNAs. We identified RRMS patients with increased leukocyte IFN-responses compared to healthy controls and other disease controls. Transfection of RNA isolated from these blood samples recapitulated the IFN-response. RNA isolated from patient blood samples that induced an IFN-response was not ribosomal RNA (rRNA), messenger RNA (mRNA), nor microRNA (miRNA); it was dsRNA. The major dsRNA fraction isolated from patient blood samples was the Alu class of retrotransposon mobile elements and genomic loci of these transcribed Alu elements were localized in the genome near leukocyte transcriptional enhancers defined by presence of histone H3K27-acetylation marks. In vitro transcribed Alu elements recapitulate this IFN-response. We conclude that stimulation of IFN-responses in RRMS patients results from increased levels of Alu dsRNAs and perhaps LINE dsRNAs.

Table 1
Demographic characteristics of the different patient populations.

	#	AGE	GENDER	ETHNICITY	STEROIDS	DMT[b]
		(% F)	(%, C/AA/As/H)[a]	% (current)	% (current)	
MS-E	65	38 ± 10	69	69/31/0/0	46	88
MS-N	65	34 ± 8	69	80/20/0/0	0	0
MS-C	45	32 ± 6	67	71/29/0/0	0	0
NMO	5	41 ± 8	69	77/23/0/0	22	55
TM	5	36 ± 9	67	79/21/0/0	0	0
PD	5	55 ± 12	5/0/0/0	0	0	
HC	55	36 ± 11	73	73/27/0/0	0	0

Blood samples in PAXgene tubes were obtained from the following U.S sites: TN, MA, MD, NY, SC, AZ, TX, CA, samples from sites in MS, MD, NY, AZ, and CA were obtained through the Accelerated Cure Project, TN site: Vanderbilt University Medical Center. European sites: Denmark, Netherlands. Diagnosis of MS was made using the standard McDonald's criteria. MS-E: RRMS with established disease of 2–5 years duration, MS-N: RRMS at the time of initial diagnosis, treatment naïve, MS-C: patients 3–6 months after initial clinically isolated syndrome, CIS, who received a diagnosis of RRMS at a later date, NMO: neuromyelitis optica of 3–5 years duration, TM: transverse myelitis of 1–5 years duration, PD: Parkinson's disease.
Differences in age, gender and ethnicity among the different patient groups compared to HC group were not statistically different, unpaired *t*-test with Welch's correction or Fisher's exact test except for the difference in age in the PD group.
[a] C, Caucasian; AA, African American; As, Asian; H, Hispanic.
[b] DMT (disease modifying therapy): copaxone, tysabri, IVIG, cellcept, methotrexate, imuran.

2. Materials and methods

2.1. Patient populations and blood sample collection and processing

Whole blood samples (~2.5 ml) were collected in PAXGENE tubes to immediately stabilize endogenous RNA from the following patient groups: 1) patients at the indicated times after their first clinical event suggestive of presence of RRMS commonly referred to as a clinically isolated event or CIS (MS-C) who later went on to receive a diagnosis of RRMS, 2) patients at the time of RRMS diagnosis prior to onset of therapies (MS-N); 3) patients with established MS (MS-E) at the time of a clinical relapse and 3–12 months after the relapse as indicated in the figure legends (MS-relapse), 4) patients with MS-E who were relapse-free for greater than 6 months, 5) patients with neuromyelitis optica (NMO), transverse myelitis (TM), and Parkinson's disease (PD); and 6) age-and gender-matched healthy control subjects (HC), see Tables 1 and 2 for additional details. RRMS patients included in this study were not on an IFN-β therapy at the time of blood collection. Blood samples were obtained from the Accelerated Cure Project (Waltham, MA) or the Vanderbilt Multiple Sclerosis Clinic (Nashville, TN) [34,35]. All blood samples were obtained with written informed consent and relevant institutional review board approval. Total RNA was isolated from PAXGENE tubes using supplied procedures (Qiagen), including DNase digestion yielding < 1% DNA contamination in these RNA samples. Integrity of RNA samples was determined by agarose gel electrophoresis and quantitative analysis of 18S and 28S RNAs.

2.2. Cell cultures

HeLa and THP-1 transformed cell lines were obtained from American Type Tissue Collection (ATCC). RAW-Lucia™ cells were from Invivogen. Cells were cultured in RPMI-1640 media supplemented with 10% fetal bovine serum, 2 mM L-glutamine, 100 units/ml penicillin, and 100 μg/ml streptomycin in 5% CO_2 in air at 37 °C.

Table 2
Characteristics of the RRMS patient population during the relapse phase.

Pt ID	Gender/Age	Symptom onset (weeks)[a]	MRI month 0	Clinical Exam month 0	ster-oids	DMARD before relapse	DMARD after relapse	MRI month 12–15	Clinical Exam month 12–15
1	m/39	4	new enhancing lesions brain	left leg weakness	yes	fingol-imide		resolution of enhancing lesions	unchanged
2	f/22	3	unchanged from previous	left arm numbness	no	nataliz-umab	nataliz-umab	unchanged from previous	Normal sensory exam
3	m/38	?	unchanged from previous	decreased sensation, arm & leg	no	none	glatimer acetate	unchanged from previous	decreased sensation, arm & leg
4	f/34	6	new T2 lesions, brain & C-spine	ataxia of gait	no	nataliz-umab	nataliz-umab	T2 lesions decreased in size & number	unchanged
5	m/43	8	new T2 lesions, C-spine	decreased sensation hands & feet	no	nataliz-umab	nataliz-umab	unchanged from previous	unchanged
6	f/38	1	new enhancing lesion, brain	mild numbness left side	yes	terifluni-mide	terifluni-mide	MRI lesions resolved	normal sensory exam
7	f/34	1	new enhancing lesion, brain	un-changed	no	fingol-imide	fingol-imide	new enhancing lesion, brain	new onset left side numbness
8	f/32	8–12	new enhancing lesion, brain	bilateral leg weakness, ataxia	yes	glatimer acetate	fingol-imide	not done	–
9	f/24	8	multiple new enhancing lesions	ataxia of gait	yes	none	nataliz-umab	stable T2 lesions	unchanged
10	m/40	1	unchanged from previous	drags left leg	yes	nataliz-umab	nataliz-umab	not done	unchanged
11	f/23	12	unchanged from previous	decreased sensation in hand	no	nataliz-umab	nataliz-umab	stable	sensory changes improved
12	m/36	12	new enhancing lesions, brain, spinal cord	decreased sensation in hand	no	glatimer acetate	nataliz-umab	new lesions	unchanged
13	f/33	4	new lesion, left internal capsule	right-sided weakness & ataxia	yes	glatimer acetate	nataliz-umab	MRI lesions resolved	right-sided weakness resolved
14	m/45	2	unchanged from previous MRI	right leg weakness & ataxia	yes	glatimer acetate	nataliz-umab	unchanged from previous MRI	unchanged

[a] Weeks before clinical and MRI evaluations.

2.3. RNA isolation from cell cultures, cDNA synthesis and PCR

Total RNA was isolated with TRI-Reagent (MRC) and purified with the RNeasy MinElute Cleanup kit (Qiagen) using an on-column DNAse treatment to ensure absence of genomic DNA contamination. cDNA was synthesized from total RNA using the SuperScript III First-Strand Synthesis Kit (Life Technologies) using oligo-dT primers and purified using the Qiagen QiaQuick PCR purification kit. Transcript levels were determined using either TaqMan assays or custom-designed primers and SYBR green as described [36]. Primers used to measure Alu and LINE elements have been described and were designed to amplify multiple Alu and LINE elements present in exons, introns and 3' untranslated regions of protein-coding genes [31]. All primer sequences used for PCR can be found in Supplementary Data File 1. Transcript levels were also determined using Power SYBR Green RNA-to-CT 1-Step Kits (Thermo Fisher Scientific) following the supplied protocols. Transcript levels were normalized to GAPDH using the formula: $2^{(}$GAPDH Ct − Target RNA Ct).

2.4. Virus infection

HeLa S3 cells cultured in Dulbecco's Modified Eagle Medium supplemented with 10% fetal bovine serum, 2 mM L-glutamine, 100 units/ml penicillin, and 100 µg/ml streptomycin, and 0.25 µg/ml Amphotericin B were infected with the T3D strain of reovirus or the 2 A Chickungunya virus (ChickV) strain at a multiplicity of infection of 10 plaque-forming units per cell or phosphate-buffered saline (mock). Cultures were harvested 24 (reovirus) or 4 h (ChickV) after infection.

2.5. Cell transfections

Cells were transfected using Lipofectamine RNAiMax (Life Technologies) with RNAs as outlined in the results section following vendor-supplied protocols (Life Technologies) as described [37].

2.6. RAW 264.7 cells and luciferase measurements

RAW-Lucia™ cells, obtained from Invivogen (San Diego, CA), are RAW 264.7 macrophage-like cells expressing the luciferase gene under the control of an IFN-stimulated response element (ISRE). Reporter cells were transfected with RNA or mock transfected and cultured for 24 h. After harvest, luciferase activity was measured as described using a TD20/20 luminometer [38]. Results are expressed as relative light units.

2.7. RNA fractionation

RNAs isolated from individual blood samples (200 ng in 10 µl) were separated into rRNA+ and rRNA-fractions using RiboMinus purification kits (Thermo Fisher Scientific), into polyA (+) and polyA (-) fractions using DynaBeads mRNA purification kits (Thermo Fisher Scientific), into < 200 bp microRNA+ (miRNA) and > 200 bp microRNA-fractions using miRNA isolation kits (QIAGEN) according to supplied protocols and into dsRNA+ and dsRNA-fractions by performing RNA-immunoprecipitations (RIP) essentially as previously described [36] using the J2 antibody specific for dsRNA greater than 40 bp in length (Scicons) [39]. Each resulting fraction obtained from the positive and negative purification was precipitated with isopropanol, rinsed, and re-suspended in 10 µl of H_2O. Each RNA fraction was independently transfected into the RAW-Lucia reporter cells. After 24 h of culture, luciferase activity was determined as above.

2.8. RNA-seq sample preparation and data analysis

RNA from patient blood collected in PAXGENE tubes was purified as described above. Library preparation was performed using the Illumina

Tru-Seq Stranded Total RNA kit. The Vanderbilt Technologies Center for Advanced Genomics (VANTAGE) performed whole genome RNA sequencing. An Illumina NovaSeq500 instrument was used to produce 100-bp paired-end reads. Quality control steps were used to evaluate raw data, alignment, and expression quantification. RNA-seq data were trimmed to remove all bases below quality, and adapter sequences were removed using trimmomatic [40]. Trimmed reads were aligned to Hg19 reference genome using RSEM [41], and counts aligned to genomic locations were used for analysis. The EdgeR package for R was used to analyze count files [42]. Data from individual samples were normalized within EdgeR and analyzed using the generalized linear model (GLM). A search for intra-host virus sequences was performed using VirusFinder, a software tool to search for virus sequences in next generation sequence data. Definition of repeat elements in the human genome was from 'repeatmasker' [43]. Differentially expressed repeat elements measured using Cufflinks/Cuffdiff were determined and expressed as read counts. A cutoff of a mean of 10 read counts in the MS-C or HC cohort or both was employed to define a repeat element as being expressed. Results from the GRCh37/hg19 builds are presented to permit a more direct comparison with previously described transcriptional enhancer (TE, SE) locations, which are also derived from the GRCh37/hg19 build.

2.9. Statistical analysis

Unless otherwise indicated, data are expressed as the mean ± SD of three or more independent experiments. Significance of two population comparisons was determined using unpaired t tests with Welch's correction for non-equal variances. Fisher's exact test was used for the analysis of contingency tables as described in the results section and figure legends. Spearman's correlation analysis was used to calculate correlation coefficients, r, and statistical significance was determined by Gaussian approximation. Unless otherwise indicated (for example, after correction for false discovery rates (FDR)), a $P < 0.05$ was considered significant. Q values were determined using the Benjamini and Hochberg formula to correct for multiple comparisons, $Q < 0.05$ was considered significant.

3. Results

3.1. IFN-responses in RRMS

We previously obtained blood samples from RRMS patients, healthy controls (HC), and disease controls, neuromyelitis optica (NMO), transverse myelitis (TM), isolated RNA, and performed whole genome RNA-sequencing (RNA-seq) with the goal of identifying protein-coding genes differentially expressed at the earliest stages of RRMS [44]. We compared the following cohorts of RRMS patients: MS-C (patients who had a previous clinical event suggestive of de-myelination, clinically isolated syndrome, CIS, and who received a diagnosis of RRMS at a later date), MS-N (patients at the time of RRMS diagnosis but treatment naive), and MS-E (patients with RRMS of a duration of 2–5 years without evidence of a clinical relapse in the last 6 months) (Table 1). We identified a subset of genes over-expressed in the MS-C and MS-N cohorts and to a lesser extent in the MS-E cohorts (Fig. 1 A,B). Several of these genes were known to also be induced by IFNs [13]. Therefore, we measured expression levels of three known IFN-response genes, *DDX58, EIF2AK2,* and *IFIT3*, in additional blood samples from these same cohorts and additional disease cohorts, NMO and TM, as well as MS-E patients with established disease but during the relapse phase of disease (Table 2). We found increased expression of each gene, *DDX58, EIF2AK2,* and *IFIT3*, in the MS-C, MS-N, and MS-relapse cohorts but not MS-E, NMO, and TM cohorts (Fig. 2 A-C). Expression levels of *DDX58, EIF2AK2* and *IFIT3* were highly correlated across the MS-C patient cohort further supporting the notion that expression of these genes was regulated by a common stimulus (Fig. 2 D,E).

3.2. IFN-responses in RRMS mediated by endogenous RNA

Intracellular sensors that induce expression of IFNs, RIG-I, MDA5 and TLR3, all recognize dsRNA. We infected HeLa cells with the reovirus T3D strain, a dsRNA virus, or the Chikungunya (Chikv) 2 A strain, a single-stranded RNA (ssRNA) virus, harvested cells and measured induction of genes induced at MS-C and MS-N phases of disease. We found that infection of HeLa cells with the reovirus T3D strain, but not the Chickv 2 A strain, also induced this same set of genes (Fig. 3A). We isolated RNA from uninfected, reovirus T3D infected, or Chickv 2 A infected HeLa cells and transfected these individual RNAs (200 ng/culture) into naïve HeLa cells. Transfection of RNA from reovirus T3D infected, but not Chickv 2 A infected or uninfected cells, resulted in a marked increase genes induced at the MS-C and MS-N phases of disease (Fig. 3B). Thus, transfection of RNA from reovirus T3D infected HeLa cells into naïve cells also stimulated expression of IFN-response genes.

To further characterize regulation of the set of genes induced at the MS-C, MS-N, and MS-relapse phases of disease, we stimulated HeLa cells with poly I/C, a dsRNA TLR3 agonist, IFN-α, IL-1β, IL-18 or IFN-γ or combinations thereof. Poly I/C and IFN-α induced expression of the known IFN-response genes, IFIT3, DDX58, PLSCR1, EIF2AK2, B2M, and CEPB5L (Fig. 3C). Under these conditions, IL-1β or IL-18 or combinations of IL-1β and IL-18 did not induce these IFN-response genes. However, IL-1β induced increased expression of a subset of other genes in this panel, *MICAL2, FGD4, RNF13, LPAR6 and SERTAD3*. IL-1β and IL-18 are products of inflammasome activation. Treatment with IFN-γ also induced increased expression of IFIT3, DDX58, PLSCR1, EIF2AK2, and B2M in HeLa cells. As a control experiment, we isolated RNA from poly I/C-, IFN-α- or IFN-γ-treated HeLa cells and transfected these RNAs into naïve HeLa cells. Transfection of these RNAs into naïve HeLa cells did not result in increased expression of these IFN-response genes (Fig. 3D). We take this to indicate that the increased expression of IFN-response genes observed above (Fig. 3B) after transfection of RNAs from infected cells is not simply the result of increased abundance of these mRNAs in the transfected RNA. In the THP-1 monocyte-like cell line, both IFIT3 and DDX58 were also induced by IFN-α, but not by IL-18, IL-1β or TNF-α (Supplementary Data File 2).

We measured expression levels of additional IFN-response genes, DDX58, IFIT3, IFI6, IFIT1 and IRF7 and found they were also induced in HeLa cells by reovirus T3D infection (Supplementary Data File 3A) or by transfection of RNA isolated from reovirus infected HeLa cells into naïve HeLa cells (Supplementary Data File 3B). Given these results, we sought to determine whether RNA isolated from blood of RRMS patients was also capable of inducing a similar IFN-response (Fig. 4A–C). Patient blood samples were obtained at the time of the first clinic visit after relapse and at several additional time points after relapse (Table 2). We also examined RNAs from the MS-C cohort (Table 1), RNA samples from patients with RRMS who had not experienced a relapse in the last 6 months (MS-E), and patients with neuromyelitis optica (NMO), transverse myelitis (TM), or Parkinson's disease (PD) (Table 1). As above, individual RNAs (200 ng/culture) were transfected into naïve HeLa cell cultures. We created an expression index to show levels of induction of IFN-response genes by comparing levels of induction by RNA isolated from these patient samples to those of RNAs isolated from HC. Transfection of RNAs isolated from the majority of MS-E patients during the relapse-remission phase of disease induced a robust increase in expression of IFN-response genes in HeLa cells (Fig. 4A). Transfection of RNAs isolated from the majority MS-C patients also induced a robust increase in expression of IFN-response genes in HeLa cells (Fig. 4B) In contrast, RNA from MS-E patients not undergoing relapse or from patients with other inflammatory or non-inflammatory neurologic disorders, NMO, TM or PD, did not induce increased expression of IFN-response genes after transfection into HeLa cells (Fig. 4C). Thus, leukocyte RNA isolated from the majority RRMS patients during the relapse phase of disease and the MS-C phase of disease induced IFN-response genes when transfected into naïve HeLa cells. In contrast

A. expression, whole blood	IFIT3	DDX58	PLSCR1	EIF2AK2	PDPR	B2M	CEP85L	MICAL2	FGD4	RNF13	LPAR6	SERTAD3	CPEB2	ANK1	TNFSF13B	LMBRD2	EXOC6	CDC137	ZFP69B
HC, avg	0.151	0.048	0.327	0.024	0.008	7.620	0.011	0.012	0.041	0.060	0.011	0.050	0.005	0.061	0.319	0.065	0.083	0.032	0.009
HC, stdev	0.201	0.084	0.508	0.021	0.006	6.046	0.008	0.021	0.023	0.036	0.014	0.026	0.004	0.048	0.205	0.042	0.042	0.016	0.011
MS-C, avg	0.304	3.381	1.448	0.087	0.034	16.66	0.051	0.098	0.426	0.145	0.047	0.118	0.735	0.185	2.054	24.61	0.265	0.069	0.019
MS-C, stdev	0.454	1.952	1.832	0.108	0.027	18.42	0.083	0.118	0.657	0.169	0.067	0.128	1.861	0.205	3.357	40.62	0.317	0.081	0.023
MS-N, avg	0.472	0.272	0.586	0.118	0.014	10.26	0.018	0.027	0.084	0.081	0.027	0.081	0.021	0.172	1.111	1.111	0.155	0.046	0.015
MS-N, stdev	0.552	0.356	1.247	0.146	0.012	12.11	0.016	0.033	0.119	0.063	0.052	0.116	0.049	0.194	1.567	2.482	0.239	0.059	0.019
MS-E, avg	0.139	0.068	0.405	0.034	0.012	11.53	0.012	0.015	0.047	0.091	0.018	0.065	0.016	0.261	0.422	0.075	0.095	0.036	0.010
MS-E, stdev	0.192	0.102	0.583	0.048	0.015	10.75	0.017	0.018	0.031	0.099	0.021	0.034	0.022	0.294	0.337	0.054	0.117	0.024	0.012
B. CASE/CTRL, log2																			
MS-C	1.0	6.2	2.1	1.9	2.1	1.1	2.2	3.0	3.4	1.3	2.1	1.2	7.3	1.6	2.7	8.6	1.7	1.1	1.1
MS-N	1.6	2.5	0.8	2.3	0.8	0.5	0.7	1.2	1.0	0.4	1.3	0.7	2.0	1.5	1.8	4.1	0.9	0.5	0.7
MS-E	-0.1	0.5	0.3	0.5	0.6	0.6	0.1	0.3	0.2	0.6	0.7	0.4	1.8	2.1	0.4	0.2	0.2	0.2	0.1
key:		Q<0.05			no fill	Q>0.05													

Fig. 1. Genes with increased expression in early compared to established MS. **A**, Genes were identified from previous RNA-seq studies [33,44] and expression levels in whole blood determined by PCR using Taqman low density arrays (TLDA). Results are expressed as the average expression level after normalization to GAPDH levels with standard deviation (stdev). Cases include MS-C (N = 40), MS-N (N = 40), and MS-E (N = 40). **B**, Results in (A) expressed as the indicated CASE/CTRL ratios, $\log_2$. Green fill, Q < 0.05, calculated to correct for multiple testing, no fill, Q > 0.05. (For interpretation of the references to colour in this figure legend, the reader is referred to the Web version of this article.)

leukocyte RNA isolated from RRMS patients not in relapse or from patients with NMO, TM, or PD did not induce IFN-response genes when transfected into naïve HeLa cell cultures.

To further explore this notion, we turned to a transformed murine macrophage (RAW264.7) reporter cell line expressing the luciferase gene under the control of an IFN-stimulated response element (ISRE). We transfected different amounts of RNA isolated from MS-C patient (N = 20) or HC (N = 20) leukocytes and measured luciferase activity expressed by the reporter cell line. We found a marked increase in luciferase activity after transfection of RNA isolated from certain MS-C patient leukocytes (designated as MS-C 1–9) but not from other MS-C patient leukocytes (designated MS-C 10–20) or from the HC leukocyte cohort (Fig. 5A). A summary of these results demonstrated that a minimum of 20 ng RNA from the MS-C 1–9 group yielded a statistically significant ~ 5-fold increase in ISRE activity compared to the HC group (Fig. 5B). We used > 5-fold increase in luciferase activity after RNA transfection as a cut-off to assign an individual patient as positive or negative for ability to activate the ISRE. We found that transfection of RNA from 9 of 20 MS-C patient leukocytes resulted in an increase in luciferase activity of > 5-fold while transfection of RNA from 0 of 20 HC leukocytes resulted in an increase in luciferase activity of > 5-fold (Fig. 5C). This frequency is similar to what we observed by directly examining induction of IFN-responsive genes by RNA isolated from the MS-C cohort (Fig. 4).

3.3. Alu and LINE dsRNAs and IFN-responses

To further characterize this RNA activity, five separate MS-C sample RNAs (MS-C #2, MS-C #5, MS-C #7, MS-C #8, MS-C#9, from Fig. 5) with high ISRE inducing activity and five separate HC sample RNAs

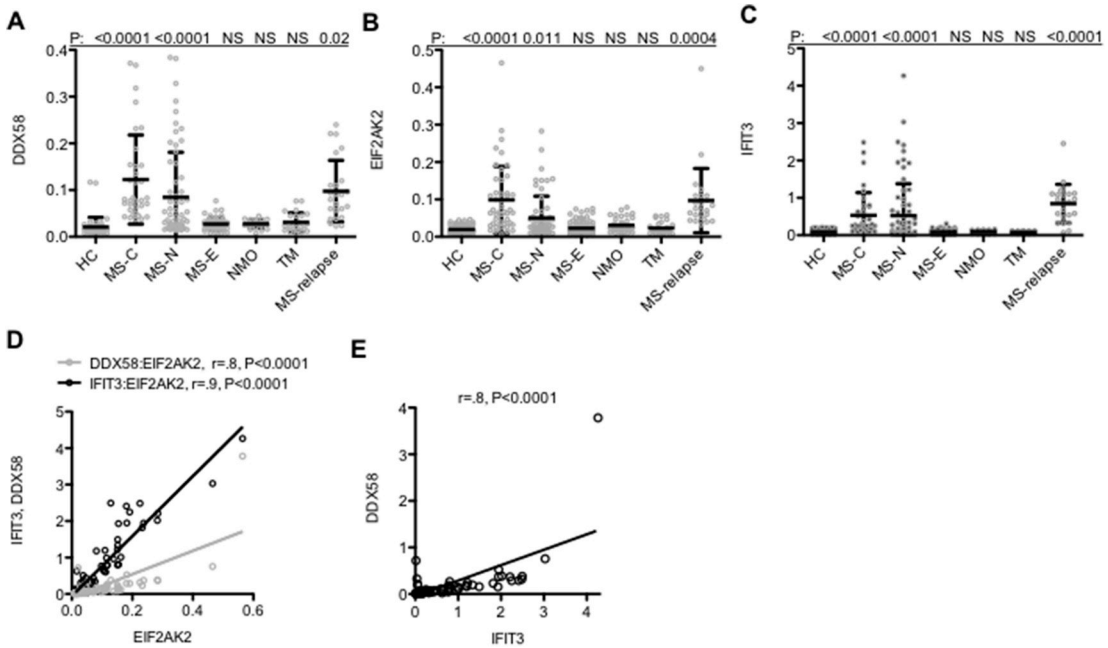

Fig. 2. Increased expression of IFN-response genes, *DDX58, EIF2AK2*, and *IFIT3* in RRMS. **A**, Expression levels of *DDX58* in peripheral leukocytes from the indicated cohorts of patients: HC: N = 40, MS-C: N = 30, MS-N: N = 30, MS-E, N = 30, NMO: N = 20, TM: N = 20, MS-relapse: N = 24, determined by RT-PCR. Y-axis is expression level of the indicated gene after normalization to *GAPDH*. **B**, As in (A), except levels of *EIF2AK2* were determined, **C**, As in (A), except levels of *IFIT3* were determined. P values were determined relative to the HC cohort using the unpaired *t*-test with Welch's correction. **D & E**, Spearman correlation analysis of expression levels of *IFIT3* or *DDX58* and *EIFAK2* and of *IFIT3* and *DDX58* in the MS-C cohort, r is the Spearman's correlation coefficient and P values determined by Gaussian approximation.

A. ratio, log2	IFIT3	DDX58	PLSCR1	EIF2AK2	PDPR	B2M	CEP85L	MICAL2	FGD4	RNF13	LPAR6	SERTAD3	CPEB2	ANK1	TNFSF13B	LMBRD2	EXOC6	CCDC137	ZFP69B
reovirus T3D*	8.7	9.5	4.7	1.3	0.7	2.5	1.8	0.6	2.1	1.4	1.8	1.3	1.4	2.2	2.7	1.4	0.5	1.1	1.3
Chikv 2A*	-0.6	0.5	-0.9	-0.3	0.2	-1.1	-1.5	-0.8	-0.1	0.0	0.1	-0.1	-0.2	0.5	-1.4	0.5	0.6	-0.7	0.1
B. ratio, log2																			
HeLa RNA (vehicle)*	0.2	-0.2	-0.3	-0.2	0.3	-0.2	0.0	-0.2	0.1	-0.3	-0.3	0.2	-0.4	-0.2	-0.1	-0.4	-0.1	0.0	-0.8
HeLa RNA (T3D reovirus)	8.2	8.3	4.2	2.8	0.8	0.6	3.0	0.7	2.6	0.5	0.9	1.8	3.2	0.9	0.3	1.5	0.8	1.7	2.4
HeLa RNA (Chickv2A)*	0.2	0.1	-0.3	-0.1	0.1	0.1	0.2	-0.2	0.1	-0.1	-0.1	0.1	0.1	0.1	-0.1	0.1	-0.1	0.3	0.1
C. ratio, log2																			
poly I/C (long)*	5.0	5.6	4.2	2.6	2.3	1.1	1.6	0.2	-0.1	0.1	-0.2	0.1	0.1	-0.1	-0.2	-0.2	0.0	0.2	0.2
IFN-α*	6.2	6.1	1.8	1.8	1.1	0.7	0.8	0.5	-0.6	0.3	-0.1	0.3	0.2	0.2	0.3	-0.6	0.3	-0.2	0.1
IL-1β*	0.1	1.9	-1.2	-0.2	0.4	0.5	0.3	7.2	2.8	1.7	1.1	1.1	0.0	-1.3	0.7	-0.7	0.2	0.2	-0.5
IL-18*	0.1	-0.1	-0.7	-0.3	1.3	0.1	0.4	0.0	0.4	0.8	1.2	-0.1	0.1	-0.1	0.5	-0.2	-0.1	0.3	-0.3
IFN-α+ IL-1β*	6.6	7.7	2.5	2.8	1.6	1.5	1.1	1.2	0.7	0.8	0.6	0.2	1.4	0.8	0.7	0.3	0.2	0.7	0.4
IFN-α+ IL-18*	7.1	7.1	2.1	2.9	0.5	1.3	0.7	1.0	0.5	0.1	1.2	0.0	1.2	1.2	0.8	0.3	0.6	0.6	0.5
IL-1β +I L-18*	0.5	1.6	-0.6	-0.2	0.8	0.2	0.7	1.0	1.3	0.4	2.2	0.6	1.2	0.7	0.4	0.0	0.0	0.4	1.4
IFN-α+ IL-1β + IL-18*	6.8	6.4	1.6	2.4	0.7	0.9	0.9	-0.7	3.3	-0.4	2.7	0.9	0.7	-0.3	1.0	-0.6	0.6	-0.2	1.4
IFN-γ*	3.2	2.2	1.1	1.5	0.8	0.9	0.1	0.4	0.1	0.2	0.3	-0.2	0.1	-0.3	-0.1	0.1	0.3	0.4	0.2
D. ratio, log2																			
poly I/C (long)*	0.2	0.1	-0.3	0.1	-0.1	0.2	0.1	-0.2	-0.1	0.2	0.3	-0.1	0.2	0.3	0.1	-0.3	-0.1	-0.2	-0.1
IFN-α*	0.2	0.1	-0.3	-0.1	-0.4	0.3	0.1	0.2	-0.1	0.1	0.3	-0.5	-0.4	-0.2	-0.1	0.1	0.3	0.4	-0.2
IFN-γ*	0.3	-0.2	0.1	0.4	-0.3	0.2	0.3	0.1	-0.2	0.3	0.1	0.2	-0.2	-0.1	0.2	0.3	-0.2	0.3	0.2
key:		Q<0.05			no fill	Q>0.05			*average ≥3 independent experiments										

Fig. 3. Genes elevated in MS-C and MS-N cohorts are also induced by activation of dsRNA sensors. **A**, HeLa cells were infected with the dsRNA virus, reovirus T3D, or the ssRNA virus, Chikungunya (Chickv2A). Cultures were harvested after 24 h (reovirus) or 4 h (ChickV2A due to the greater cytopathic effects), RNA isolated, and expression levels of indicated genes determined by PCR. Results are expressed as ratios of gene expression, infected/uninfected cultures, $\log_2$ after normalization to *GAPDH*. **B**, RNA (200 ng/culture) isolated from uninfected HeLa cells, HeLa cells infected with T3D reovirus, or HeLa cells infected with ChickV2A virus was transfected into naïve HeLa cells using lipofectamine. Cultures were harvested after 24 h and expression levels of indicated genes determined by PCR. Results expressed as in (A) relative to mock-transfected HeLa cultures. **C**, HeLa cells were treated with the TLR3 agonist, poly I/C, IFN-α, IL-1β IL-18, IFN-γ or combinations thereof. Cultures were harvested after 24 h and expression levels of indicated genes determined by PCR. Results expressed as in (A) relative to untreated HeLa cultures. **D**, RNA was isolated from HeLa cells after 24 h of treatment with either poly I/C, IFN-α, or IFN-γ and transfected into naïve HeLa cells. RNA was isolated from transfected cells and levels of indicated genes determined by PCR. Results are expressed as in (A) relative to untreated HeLa cultures. Green fill, $Q < 0.05$, calculated to correct for multiple testing. (For interpretation of the references to colour in this figure legend, the reader is referred to the Web version of this article.)

with low ISRE inducing activity were selected. Our rationale for using this smaller number of samples was that our goal was to characterize the properties of the ISRE-inducing activity present in these RNA samples. Individual total RNAs were transfected into ISRE reporter cell cultures (200 ng/culture) to measure total ISRE inducing activity present in the RNA sample. RNA samples (200 ng) were individually fractionated into rRNA and non-rRNA fractions, polyA (+) and polyA (-) RNA fractions, > or < 200 bp RNA fractions, or dsRNA and ssRNA fractions separated by immunoprecipitation using the J2 antibody as described in the methods section, *2.6* RNA *fractionation*. Total amounts

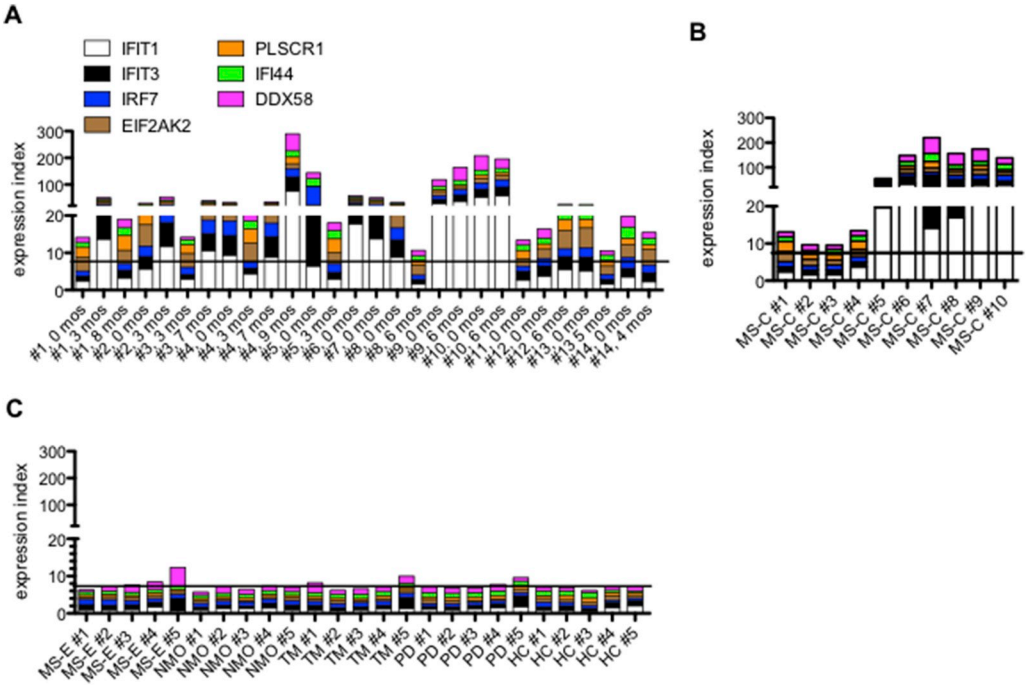

Fig. 4. Induction of IFN-response genes by RRMS patient RNA. **A**, RNA was isolated from whole blood from MS patients experiencing a relapse (0 months) and at the indicated times after relapse. Total RNA (200 ng) from individual patient or HC samples was transfected into naive HeLa cell cultures. After 24 h, RNA was isolated from transfected cells and levels of the indicated IFN-response genes determined by PCR. We expressed results as an expression index created by summing gene expression induced by individual patient RNAs to the average induction by 5 individual HC RNAs. **B**, As in (A) except RNAs were isolated from the MS-C cohort. **C**, As in (A) except RNAs were obtained from MS-E, NMO, TM, or PD patients or HC. Solid lines identify average HC index = 7. Statistical significance was determined by using the Benjamini and Hochberg formula to correct for multiple comparisons, $Q < 0.05$ was considered significant. **A**, MS-relapse versus HC: $Q < 0.0001$, **B**, MS-C versus HC: $Q = 0.01$, and **C**, MS-E versus HC: $Q > 0.05$, NMO versus HC: $Q > 0.05$, TM versus HC: $Q > 0.05$, and PD versus HC, $Q > 0.05$.

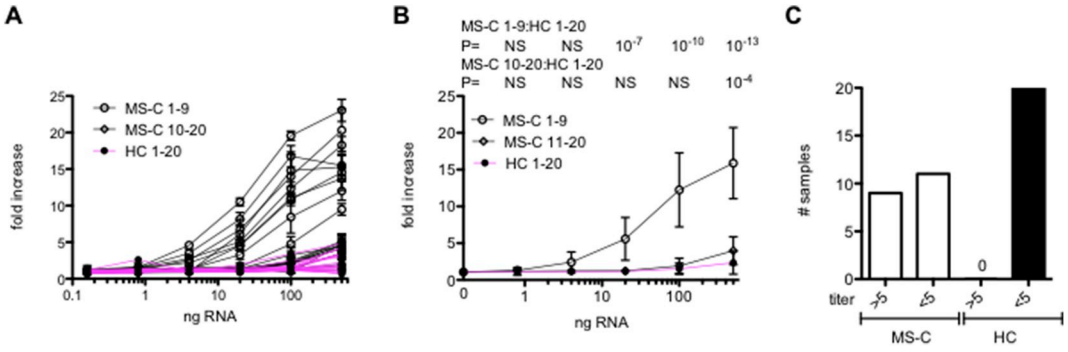

Fig. 5. MS-C RNA-mediated ISRE activation. **A**, The indicated amounts of RNA isolated from MS-C patient (N = 20) or HC (N = 20) blood samples were transfected into the RAW-Lucia™ reporter cell line expressing the luciferase gene under the control of an ISRE. After 24 h, luciferase activity determined. Results are expressed as fold increase in luciferase activity compared to mock-transfected controls in triplicate; MS-C 1–9 induced maximum fold increase of 10–25 (open circles, black line), MS-C 10–20 induced maximum fold increase of 1–5 (open diamonds, black line), and HC 1–20 (closed circles, magenta line) induced maximum fold increase of 1–5. **B**, Averages, standard deviations and unpaired T test with Welch's correction of results in A. **C**, Results from A are expressed as the number of MS-C samples or HC samples that induced a > 5-fold increase in luciferase activity above the mock-transfected control. $P = 0.001$, Fisher's exact test.

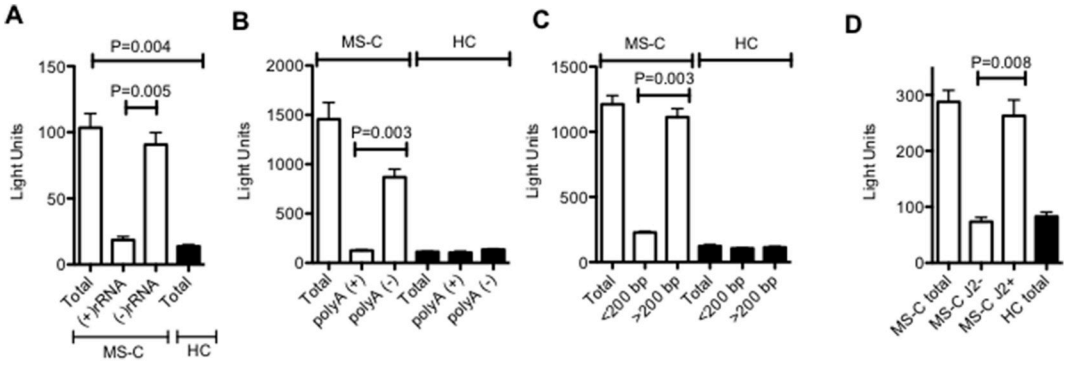

Fig. 6. Characterization of MS-C RNA ISRE-inducing activity. Five MS-C RNAs with high ISRE-inducing activity and five HC RNAs with low ISRE-inducing activity (200 ng each) were selected (Fig. 5) and individually tested for ISRE-inducing activity. These RNAs were separated into **A**, (+) rRNA and (-) rRNA fractions, **B**, polyA (+) and polyA (-) fractions, **C**, fractions of < or > 200 nucleotide lengths, and **D**, J2- (dsRNA-) and J2+ (dsRNA+) fractions as outlined in methods and re-analyzed for ISRE inducing activity. Total indicates the ISRE inducing activity of the unfractionated sample. Equivalent volumes of each fraction were transfected into the RAW-Lucia reporter cells. After 24 h, luciferase activity was determined, Y-axis = relative light units. P values were determined using the unpaired T test with Welch's correction.

of Isolated fractions were transfected into the ISRE reporter cell line. We found that the ISRE-inducing activity isolated from MS-C patient leukocytes segregated with the non-rRNA fraction, the polyA (-) RNA fraction, the > 200 bp fraction, and the dsRNA fraction (Fig. 6A–D). Taken together, these results indicate that the RNA that stimulates the ISRE response found in MS-C leukocytes is a dsRNA but not rRNA, mRNA or a small RNA such as a microRNA.

We performed whole-genome RNA-seq to identify RNAs present in the dsRNA fraction. Total RNA from 3 HC to 3 MS-C samples was depleted of rRNA, and dsRNA was isolated by immunoprecipitation using the J2 antibody. A search for intra-host virus sequences using VirusFinder did not reveal significant differences between MS-C and HC dsRNA samples [45]. As a first step, we used the Integrative Genomics Viewer, IGV, Broad Institute, a high-performance tool to visualize genomic data [46]. We compared total polyA (+) RNA to dsRNA from MS-C leukocytes obtained from RNA-seq analysis (Fig. 7A). As an illustrative example, we compared read counts in the polyA (+) fraction to the dsRNA fraction of one MS-C patient leukocyte RNA sample at the *CSF3R* gene (tracks 1–3). In the polyA (+) faction, exons were highly expressed with evidence of some intron retention between exons 3–4, 6–7, and 12–13 [33]. In the dsRNA fraction, we found absence of CSFR exon transcripts, confirming purity of our dsRNA preparations, and high levels of transcripts between exons 3–4. This genomic region was also rich in Alu and LINE elements (track 4). This overlay also indicates that the Alu elements were expressed at higher levels than the LINE elements. In contrast, upstream Alu elements were only weakly expressed (at ~36,934 kb and ~36,936 kb, chr1). Other highly expressed mRNAs, such as *GAPDH*, were also not detected in the dsRNA samples. Thus, we determined levels of expression of repeat elements using the repeatmasker definition list (http://www.repeatmasker.org) [43]. Roughly, there are about 1,000,000 Alu elements, 1,000,000 LINE elements, and 2,000,000 other repeat elements in the human genome [29,30,43]. Using a cutoff of average > 10 read counts from all six RNA-seq analyses, three MS-C and three HC samples, as a lower limit of detectable and reproducible RNA expression of Alu, LINE and other repeat elements, we determined that about 400,000 Alu elements, 67,000 LINE elements and 62,000 other repeat elements were expressed in our samples (Fig. 7B). Also, a greater number of Alu elements exhibited higher expression levels than the LINE and other repeat elements with about 10,000 Alu elements expressed at > 500 read counts while < 1000 LINE and < 1000 other repeat elements were expressed at > 500 read counts (Fig. 7C). Alu elements are divided into major classes termed AluJ elements originating about 65 million years ago, AluS elements originating about 30 million years ago, and the younger AluY elements. Multiple sub-classes exist within each class. Of these, more AluS elements exist in the genome and proportionately more expressed AluS elements were identified by our analysis (Fig. 7D, see also Supplementary Data File 4 for more detail). Of the LINE elements, the L1 class had the greatest number of highly expressed LINE elements (Fig. 7E). We also determined locations in the genome of expressed Alu and LINE elements using the > 10 read count cutoff. Greater than 80% of expressed Alu and LINE elements were located in introns of protein-

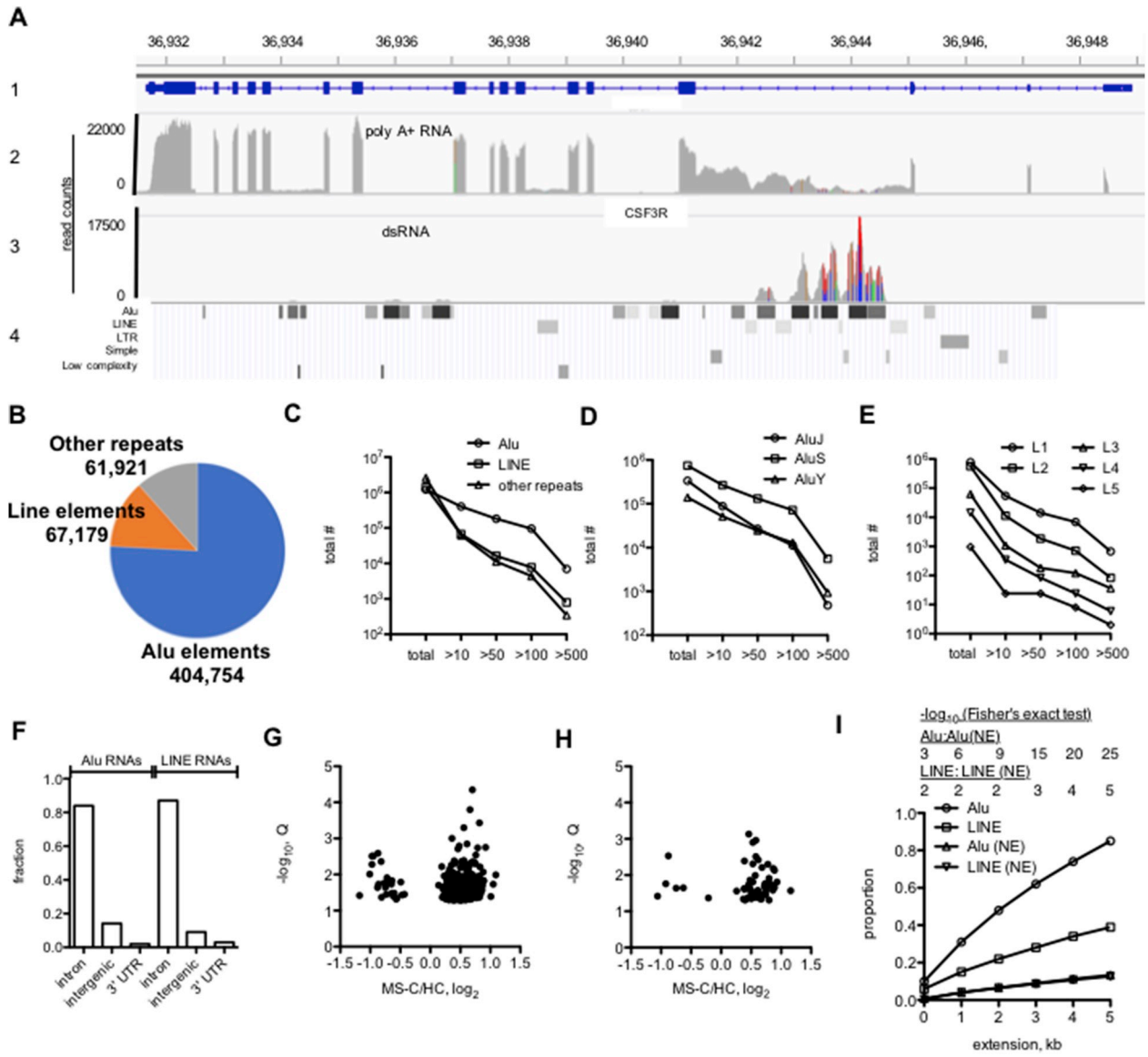

Fig. 7. Analysis of leukocyte dsRNA content by whole genome RNA-seq. **A**, Integrative Genomics Viewer (IGV) RNA-seq tracks. The first track (1) shows genomic coordinates of the CSF3R gene, chr 1 with exons and introns. The second track (2) shows levels of polyA (+) mRNAs in read counts from one MS-C RNA sample [33]. The third track (3) shows dsRNA levels in read counts from one MS-C sample. The fourth track (4) shows positions of Alu, LINE, LTR and other repeat elements (repeatmasker). Results presented in **B-E** were calculated from the average of three MS-C and three HC samples **B**, Pie chart showing number of Alu, LINE and other repeat elements in the human genome expressed in leukocytes in the dsRNA + fraction with average read count > 10. **C-E**, Distribution of repeat element RNAs expressed at > 10, > 50, > 100, > 500 average read counts compared to total number of repeat elements in the human genome. **C**, Alu, LINE, other repeats, **D**, J, S, Y classes of Alu elements, **E**, L1-L5 classes of LINE elements. **F**, Fraction of total expressed Alu and LINE RNAs (average read count > 10) transcribed from introns of protein-coding genes, from intergenic space, or from 3′ UTR of protein coding genes. **G**, **H**, 'Volcano plots' showing differential expression of Alu (**G**) and LINE(**H**) RNA elements (> 500 read count) between MS-C and HC cohorts, Q < 0.05. **I**, Genomic locations of highly expressed Alu and LINE elements (> 500 read count) are near leukocyte transcriptional enhancers. Y-axis shows the proportion of highly expressed Alu and LINE elements with genomic locations within the indicated genomic distance of a leukocyte enhancer, X-axis. P values, $-\log_{10}$, shown above the graph were determined using Fisher's exact test.

coding genes, about 10% were located in intergenic genome space and about 1–2% were located in 3' untranslated regions of protein-coding genes (Fig. 7F). We also determined if highly expressed Alu and LINE elements (> 500 read counts) were differentially expressed between MS-C and HC samples. Of both highly expressed Alu and LINE elements, more were expressed at higher levels in the MS-C samples than the HC samples (Fig. 7G and H). Thus, we found that expressed Alu and LINE elements were abundant in the genome, were mostly found in introns of protein-coding genes, exhibited variable levels of expression, and a number of the highly expressed Alu and LINE elements were expressed at higher levels in the MS-C cohort than the HC cohort.

In addition to genes, enhancer regions in the genome identified by epigenetic markings are heavily transcribed [47–51]. These RNAs are categorized as 1-directional (1D-eRNA) or 2-directional (2D-eRNA) RNAs depending upon if they are transcribed from a single DNA strand (1D-eRNA) or in both sense and antisense directions (2D-eRNA), respectively. The 1D-eRNAs are greater in length (> 1 kb) than 2D-eRNAs (< 200 bp). Considering the possibility that highly expressed Alu and LINE elements may be transcribed from leukocyte enhancer regions, we compared genomic locations of leukocyte highly expressed Alu and LINE elements (> 500 read count) to genomic locations of Alu and LINE elements that were not expressed in leukocytes from our RNA-seq analysis to the genomic positions of previously reported leukocyte enhancer elements defined by epigenetic markings [47]. For this

comparison, we also extended Alu/LINE genomic lengths by 1–5 kb to determine if this affected the overlaps as the exact relationship between an enhancer region defined by epigenetic markings and transcription of 1D-eRNAs and 2D-eRNAs is incompletely understood. Performing this analysis, we found that greater than 80% of highly expressed Alu elements were within 5 kb of a leukocyte enhancer while only ~10% of Alu elements not expressed (Alu (NE)) in leukocytes were within 5 kb of a leukocyte enhancer (Fig. 7I) and this difference was highly significant. We also found that ~40% of highly expressed LINE elements were within 5 kb of a leukocyte enhancer while only ~10% of LINE not expressed in leukocytes (LINE (NE)) were within 5 kb of a leukocyte enhancer. The association between genomic positions of highly expressed LINE elements and leukocyte enhancers did not reach the same level of statistical significance as the association between genomic positions of highly expressed Alu elements and leukocyte enhancers. Taken together, these results indicate that transcribed Alu and LINE elements are located near transcriptional enhancers in the genome.

We used PCR to independently measure total levels of Alu, LINE3, RNU-1, and RNU-2, and 18S rRNA RNAs in each of five MS-C samples with high ISRE inducing activity, each of 5 MS-E samples with undetectable or low ISRE inducing activity and each of five HC samples with undetectable ISRE inducing activity. PCR primers used to measure Alu and LINE3 RNAs amplify multiple classes of Alu and LINE3 elements making it possible to obtain a general estimate of total levels of these RNAs in a biological sample. Total levels of the indicated RNAs were not different among MS-C, MS-E and HC samples (Fig. 8A). We asked if there was a difference in the dsRNA character of these RNAs between the three sample sets by isolating dsRNA using J2 antibody specific for dsRNA > 40 bp in length and determining RNA levels in bound and unbound fractions from each MS-C sample, each MS-E sample and each HC sample. We found a marked increase in the levels of Alu and LINE 3 RNA, but not RNU-1, RNU-2 and 18s rRNA, that were dsRNA in the MS-C samples compared to either MS-E or HC samples (Fig. 8B). Transcribed Alu and LINE3 elements were also localized in the cytoplasm rather than nucleus (Supplementary Data File 5). We fractionated MS-C RNA by SDS polyacrylamide gel electrophoresis and eluted RNA fractions and tested them for Alu levels by PCR and ISRE-inducing activity in the RAW264.7 reporter cells. We detected two clear peaks of Alu signal, a weaker signal at about 300 bp and a stronger signal at ~1–2 kb but only one peak of ISRE-inducing activity at ~1–2 kb (Fig. 8C). Thus, the ISRE-inducing activity co-migrated with the larger Alu size fraction, which is consistent with results above demonstrating that highly expressed Alu elements are associated with enhancers and 1d-eRNAs are ~1–2 kb in size and potentially contain multiple Alu and LINE elements. To directly test if Alu RNA activated the ISRE reporter, we transfected *in vitro* transcribed Alu RNA into RAW-Lucia reporter cells and measured luciferase activity 24 h later. We found that Alu RNA induced ISRE activity in a dose-dependent manner (Fig. 8D). We conclude from these studies that increased levels of double-stranded Alu and perhaps LINE RNAs contribute to the observed increase in ISRE-inducing activity in the MS-C RNA samples compared to the HC RNA samples.

4. Discussion

IFN-responses are elevated in RRMS patient leukocytes in early disease, MS-CIS, prior to diagnosis of RRMS, in a cohort of RRMS patients at the time of diagnosis of RRMS but prior to onset of therapies (MS-N), and during the relapse and post-relapse phase in patients with established disease, MS-relapse. RNA isolated from RRMS patient leukocytes is also capable of inducing IFN-responses in virgin cells. Further, neuromyelitis optica (NMO), transverse myelitis (TM), and Parkinson's disease (PD) are also diseases of the nervous system of unknown etiology but where inflammatory components are suspected. Leukocyte RNA isolated from these patient samples does not activate an IFN-response suggesting existence of these RNAs is not a property of all disorders of the nervous system that possess an inflammatory component. These RNAs capable of inducing IFN-responses are not polyA (+) RNAs, rRNAs, or miRNAs, but are dsRNAs. Our analysis of MS-C and HC dsRNA compartments reveals the presence of highly expressed repeat elements, most notably Alu elements. Both highly expressed Alu and LINE elements are enriched in the MS-C cohort compared to the HC cohort. Genomic loci containing highly expressed Alu and LINE elements are localized within or near leukocyte transcriptional enhancers raising the possibility that these highly expressed Alu and LINE elements are components of 1D eRNAs. Transfection of In vitro transcribed

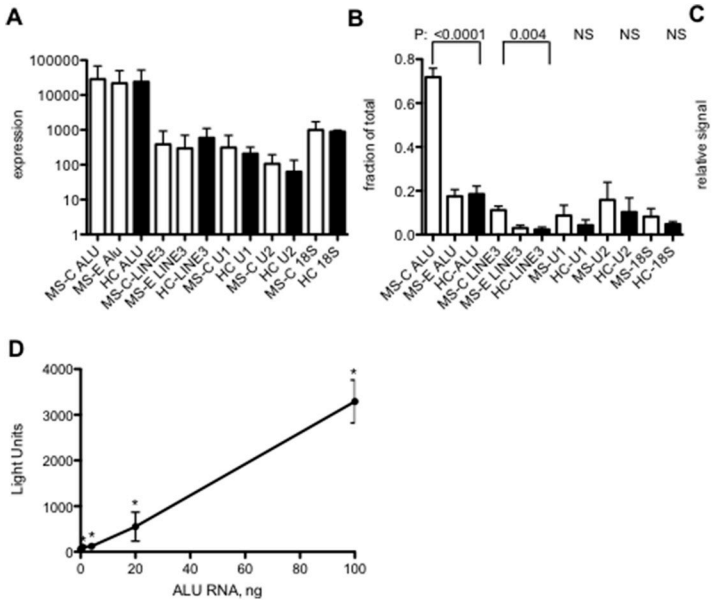

Fig. 8. MS-C Alu RNAs induce ISRE-enhancer activity. **A**, Total levels of the indicated RNAs were determined by PCR analysis of independent MS-C, MS-E and HC RNA samples (N = 5 each). RNA differences among MS-C, MS-E, and HC cohorts were not statistically significant (unpaired *t*-test with Welch's correction). **B**, Total levels of the indicated RNAs bound to the J2 antibody specific for long dsRNA were determined by PCR analysis of bound fractions and total fractions. Results are expressed as fraction of total (N = 5 each). P values are for each MS-C: HC comparison using the unpaired *t*-test with Welch's correction, NS = not significant. Differences between MS-E and HC samples were not statistically significant. **C**, MS-C dsRNA was fractionated by SDS polyacrylamide gel electrophoresis. RNA was eluted from individual fractions and tested for ISRE-inducing activity by transfection into the RAW-Lucia reporter cell line and Alu RNA quantity was determined by PCR. Relative signals, Y-axis, were calculated by converting the highest bioactivity signal to 1 and the highest Alu signal to 1 and calculating relative signals in the other fractions. X-axis is size in kb. # indicates if Alu RNA levels were significantly different from background levels, * indicates if ISRE-inducing activity was significantly different from background levels, $P < 0.05$ compared to background signal. **D**, The indicated amounts of *in vitro* transcribed Alu RNA (~300 bp in length) were transfected into RAW-Lucia reporter cells. After 24 h, luciferase activity was determined, Y-axis = relative light units. *, $P < 0.05$ compared to background luciferase signal.

Alu RNA into target cells activates an IFN-response, thus recapitulating the response of MS-C RNA. In summary, our results are consistent with a model where an imbalance of highly expressed Alu- and LINE-dsRNAs induces IFN-responses at distinct stages of RRMS.

One limitation of our study is that we do not completely address the correlation between elevated IFN-responses or elevated levels of Alu dsRNAs in RRMS and disease activity, outcomes or other clinical parameters. Our findings that RRMS patients during relapse have elevated IFN-responses compared to patients not in relapse suggest that IFN-responses and elevated levels of Alu dsRNAs correlate with relapse or recovery from relapse. However, it is not possible to make this conclusion with absolute certainty without extensive longitudinal clinical studies coupled with measurements of IFN-responses and Alu dsRNA levels. A second limitation is that we did not investigate possible sources of endogenous stimuli that might lead to increased Alu dsRNA levels and corresponding IFN-responses. Stimuli that can lead to increased levels of Alu RNAs in tissue culture models include cellular stressors such as heat shock responses, oxidative stress, inhibition of mRNA transcription or protein translation, and ionizing irradiation, as well as viral infection [14,24,52]. Thus, identifying sources of endogenous stimuli in RRMS that lead to increased Alu dsRNA levels may improve our understanding of RRMS pathogenesis.

A second limitation is that we isolated RNA from whole blood to perform these studies so it is not possible to conclude with absolute certainty if increased Alu dsRNAs found RRMS are intracellular or present in serum or both. Stimulation of IFN-responses by Alu dsRNAs requires transfection into naïve recipient cells. Thus, it seems most likely that in RRMS, intracellular Alu dsRNAs activate intracellular dsRNA sensors and stimulate increased IFN-responses via a cell intrinsic process rather than a process where Alu dsRNAs are released from one cell or present in serum and activate another cell via perhaps a cell surface receptor. However, further studies will be required to address this question.

Defects in RNA processing exist in RRMS [33]. These include mis-processing of rRNAs resulting in increased rRNA length, extensive exon loss and intron retention in mRNAs, increased poly-adenylation of rRNAs, as well as certain Y RNAs and U snRNAs. These defects result, at least in part, from reduced levels of Ro60 and La proteins in RRMS leukocytes. Ro60 and La are part of a ribonucleoprotein complex that binds mis-folded RNAs facilitating their degradation by the RNA exosome [25,27,53,54]. Ro60 also binds RNA Alu elements and thus, if these are mis-folded, Ro60 may facilitate their degradation by the RNA exosome. Increased expression of IFN-response genes, 'IFN signature', is present in numerous autoimmune diseases, most notably SLE, but also RRMS, RA, and Sj. In SLE, increased Alu RNA expression, which may result from failure of the exosome to degrade these dsRNAs, is also linked to the IFN signature. Reduced levels of Ro60 and La proteins in RRMS may also contribute to increased levels of dsRNA Alu elements in RRMS due to failure to degrade Alu RNAs. In fact, loss of Ro60 in cell lines causes increased Alu RNA expression and activates inflammatory gene expression, including IFN-α, lending further support to this notion.

Other factors exist that may govern responses of dsRNA sensors to endogenous dsRNAs such as repetitive Alu and LINE RNA elements. For example, studies suggest that the normal RNA-rich environment in cells may actually inhibit activation of the dsRNA sensor, MDA5, and perhaps additional dsRNA sensors by Alu and LINE dsRNAs, thus limiting activation of IFN responses creating a kind of state of innate immune tolerance [32]. In this regard, simple depletion of total cellular RNAs by such things as cellular stress may abrogate this inhibition or tolerance leading to activation of these sensors resulting in increased IFN responses. In addition, RNA A to I editing catalyzed by double-stranded RNA-specific adenosine deaminase (ADAR) is a known mechanism that disrupts the dsRNA character of repetitive Alu and LINE RNA elements and is thought to prevent aberrant activation of dsRNA sensors by endogenous dsRNAs [55,56]. These additional factors may contribute to the observed shifts in balances of Alu and LINE dsRNAs in RRMS and corresponding induction of IFN responses.

Further comparison between SLE and RRMS seems worthwhile. In SLE, the IFN-response is thought to be pathogenic and is increased during clinical flares [19]. In fact, treatment of patients with type 1 IFNs induces lupus-like flares in rare instances [57,58]. In contrast, therapeutic versions of IFN-β are mainstays for treatment of RRMS reducing both relapse rates and long-term disability [59–61]. Clinical trials with IFN-α have achieved similar positive clinical effects but IFN-α is not used as the standard of care for RRMS [62]. In contrast, while type 1 IFNs have positive impacts on RRMS disease pathogenesis, studies in both animal models of MS as well as human RRMS indicate that IFN-γ has a negative impact on disease pathogenesis and increases disease relapses [63,64]. The IFN-response and presence of dsRNAs that induce the IFN-response seem to peak in intensity in the MS-relapse cohort after relapse or extend significantly beyond the clinical relapse phase well into clinical remission. Taken together, these data raise the possibility that the increase in the endogenous level of Alu dsRNAs, and perhaps other dsRNAs, and the subsequent IFN-response may have a positive impact on RRMS. A better understanding of the origins and dynamics of expression of these dsRNA Alu elements may improve current disease management in RRMS and possibly lead to identification of new therapeutic targets for RRMS.

Over 1,000,000 Alu elements exist in the human genome suggesting their presence contributes to the fitness of the species. Our results show that substantial portions of Alu and LINE transcripts exist as dsRNA structures and this portion is significantly increased at discrete stages of RRMS. Transcriptional enhancers in the genome are also transcribed and produce what are termed enhancer RNAs or eRNAs. Our results show that genomic locations of highly expressed Alu and LINE RNAs are near leukocyte-specific transcriptional enhancers. The corollary is also true, Alu elements within the genome also possess tissue-specific enrichment for the enhancer epigenetic mark, H3K4me1 and certain Alu elements possess enhancer activity in reporter assays suggesting Alu elements may be critical components of enhancers [65]. Taken together our results suggest that transcription at enhancers may give rise to highly expressed Alu and LINE elements as part of an enhancer RNA or eRNA. However, further analyses of especially these longer highly expressed Alu and/or LINE structures will be required to determine the accuracy of these suggestions.

Besides their antiviral effects, IFNs also have broad anti-inflammatory properties mediated, in part, by their ability to inhibit inflammasome activity [66–68], but also by other mechanisms such as their ability to inhibit generation of antibody-producing B cells [69]. In contrast to IFNs, Alu RNAs also activate the inflammasome. Thus, Alu RNA elements may have both pro- and anti-inflammatory properties. Whether additional pathways exist that may be activated by dsRNA Alu and LINE elements is incompletely understood at present but represents an avenue of potentially important future investigation.

Author contributions

Conceptualization, T.M.A., M.J.H, C.A.P, C.F.S.; Methodology, T.M.A., J.K., M.J.H., C.A.P.; Formal Analysis, T.M.A., M.J.H., C.A.P.; Investigation, M.J.H., C.A.P., Y.Z.; Resources, S.S., T.S.D., K.M.O.; Writing-Original Draft, T.M.A., M.J.H; Writing-Review and Editing, T.M.A, M.J.H, J.K.; Supervision, T.M.A., J.K., Project Administration, T.M.A.; Funding Acquisition, TMA, TSD & CFS.

Conflicts of interest

The authors declare no competing interests.

Data and materials availability

RNA-sequencing data has been deposited in GEO with accession

number GSE126427.

Acknowledgements

We wish to thank the individuals who provided blood samples. Blood samples were obtained from the following organizations: Accelerated Cure Project, Waltham, MA, USA, Vanderbilt University Medical Center, Nashville, TN, USA, University of Copenhagen, Copenhagen, Denmark.

Appendix A. Supplementary data

Supplementary data to this article can be found online at https://doi.org/10.1016/j.jaut.2019.02.003.

Funding

This work was supported by grants from the NIH, R01AI044924, R21AI128281, and R21AI144193 (TMA), R01AI038296 (TSD) and R44AI124766 (IQuity Labs).

References

[1] R. Medzhitov, Toll-like receptors and innate immunity, Nat. Rev. Immunol. 1 (2001) 135–145.
[2] R. Medzhitov, C. Janeway Jr., Innate immune recognition: mechanisms and pathways, Immunol. Rev. 173 (2000) 89–97.
[3] D. Goubau, M. Schlee, S. Deddouche, A.J. Pruijssers, T. Zillinger, M. Goldeck, et al., Antiviral immunity via RIG-I-mediated recognition of RNA bearing 5 '-diphosphates, Nature 514 (2014) 372–375.
[4] C.A. Janeway Jr., R. Medzhitov, Innate immune recognition, Annu. Rev. Immunol. 20 (2002) 197–216.
[5] S.K. Vanaja, V.A.K. Rathinam, K.A. Fitzgerald, Mechanisms of inflammasome activation: recent advances and novel insights, Trends Cell Biol. 25 (2015) 308–315.
[6] R. Medzhitov, C.A. Janeway Jr., Innate immune recognition and control of adaptive immune responses, Semin, Immunology 10 (1998) 351–353.
[7] S.D. Der, A.M. Zhou, B.R.G. Williams, R.H. Silverman, Identification of genes differentially regulated by interferon alpha, beta, or gamma using oligonucleotide arrays, Proc. Natl. Acad. Sci. U. S. A 95 (1998) 15623–15628.
[8] D.V. Kalvakolanu, E.C. Borden, An overview of the interferon system: signal transduction and mechanisms of action, Canc. Invest. 14 (1996) 25–53.
[9] S. Pestka, C.D. Krause, M.R. Walter, Interferons, interferon-like cytokines, and their receptors, Immunol. Rev. 202 (2004) 8–32.
[10] C.A. Biron, Interferons alpha and beta as immune regulators - a new look, Immunity 14 (2001) 661–664.
[11] C.E. Samuel, Antiviral actions of interferons, Clin. Microbiol. Rev. 14 (2001) 778–809.
[12] G. Trinchieri, Type I interferon: friend or foe? J. Exp. Med. 207 (2010) 2053–2063.
[13] J.W. Schoggins, S.J. Wilson, M. Panis, M.Y. Murphy, C.T. Jones, P. Bieniasz, et al., A diverse range of gene products are effectors of the type I interferon antiviral response, Nature 472 (2011) 481–485.
[14] E.S. Lander, I.H.G.S. Consortium, L.M. Linton, B. Birren, C. Nusbaum, M.C. Zody, et al., Initial sequencing and analysis of the human genome, Nature 409 (2001) 860–921.
[15] L. Bennett, A.K. Palucka, E. Arce, V. Cantrell, J. Borvak, J. Banchereau, et al., Interferon and granulopoiesis signatures in systemic lupus erythematosus blood, J. Exp. Med. 197 (2003) 711–723.
[16] E.C. Baechler, F.M. Batliwalla, G. Karypis, P.M. Gaffney, W.A. Ortmann, K.J. Espe, et al., Interferon-inducible gene expression signature in peripheral blood cells of patients with severe lupus, Proc. Natl. Acad. Sci. U. S. A 100 (2003) 2610-2605.
[17] J. Lubbers, M. Brink, L.A.V. de Stadt, S. Vosslamber, J.G. Wesseling, D. van Schaardenburg, et al., The type I IFN signature as a biomarker of preclinical rheumatoid arthritis, Ann. Rheum. Dis. 72 (2013) 776–780.
[18] C.L. Verweij, S. Vosslamber, Relevance of the type I interferon signature in multiple sclerosis towards a personalized medicine approach for interferon-beta therapy, Discov. Med. 15 (2013) 51–60.
[19] M.K. Crow, Type I interferon in the pathogenesis of lupus, J. Immunol. 192 (2014) 5459–5468.
[20] S. Sharma, K.A. Fitzgerald, M.P. Cancro, A. Marshak-Rothstein, Nucleic acid-sensing receptors: rheostats of autoimmunity and autoinflammation, J. Immunol. 195 (2015) 3507–3512.
[21] M.J. Jimenez-Dalmaroni, M.E. Gerswhin, I.E. Adamopoulos, The critical role of toll-like receptors - from microbial recognition to autoimmunity: a comprehensive review, Autoimmun. Rev. 15 (2016) 1–8.
[22] A. Nezos, F. Gravani, A. Tassidou, E.K. Kapsogeorgou, M. Voulgarelis, M. Koutsilieris, et al., Type I and II interferon signatures in Sjogren's syndrome pathogenesis: contributions in distinct clinical phenotypes and Sjogren's related lymphomagenesis, J. Autoimmun. 63 (2015) 47–58.
[23] D.R. Ranoa, A.D. Parekh, S.P. Pitroda, X. Huang, T. Darga, A.C. Wong, et al., Cancer therapies activate RIG-I-like receptor pathway through endogenous non-coding RNAs, Oncotarget 7 (2016) 26496–26515.
[24] K.B. Chiappinelli, P.L. Strissel, A. Desrichard, H.L. Li, C. Henke, B. Akman, et al., Inhibiting DNA methylation causes an interferon response in cancer via dsRNA including endogenous retroviruses, Cell 162 (2015) 974–986.
[25] C. Belair, S. Sim, S.L. Wolin, Noncoding RNA surveillance: the ends justify the means, Chem. Rev. 118 (2018) 4422–4447.
[26] M.M. Portal, V. Pavet, C. Erb, H. Gronemeyer, Human cells contain natural double-stranded RNAs with potential regulatory functions, Nat. Struct. Mol. Biol. 22 (2015) 89–97.
[27] T. Hung, G.A. Pratt, B. Sundararaman, M.J. Townsend, C. Chaivorapol, T. Bhangale, et al., The Ro60 autoantigen binds endogenous retroelements and regulates inflammatory gene expression, Science 350 (2015) 455–459.
[28] J. Houseley, D. Tollervey, The many pathways of RNA degradation, Cell 136 (2009) 763–776.
[29] A.J. Mighell, A.F. Markham, P.A. Robinson, Alu sequences, FEBS Lett. 417 (1997) 1–5.
[30] P. Deininger, Alu elements: know the SINEs, Genome Biol. 12 (2011) 236.
[31] M. Marullo, C. Zuccato, C. Mariotti, N. Lahiri, S.J. Tabrizi, S. Di Donato, et al., Expressed Alu repeats as a novel, reliable tool for normalization of real-time quantitative RT-PCR data, Genome Biol. 11 (2010) R9.
[32] S. Ahmad, X. Mu, F. Yang, E. Greenwald, J.W. Park, E. Jacob, et al., Breaching self-tolerance to Alu duplex RNA underlies MDA5-mediated inflammation, Cell 172 (2018) 797–810.
[33] C.F. Spurlock, J.T. Tossberg, Y. Guo, S. Sriram, P.S. Crooke, T.M. Aune, Defective structural RNA processing in relapsing-remitting multiple sclerosis, Genome Biol. 16 (2015) 58.
[34] J.T. Tossberg, P.S. Crooke, M.A. Henderson, S. Sriram, D. Mrelashvili, S. Chitnis, et al., Gene-expression signatures: biomarkers toward diagnosing multiple sclerosis, Genes Immun. 13 (2012) 146–154.
[35] J.T. Tossberg, P.S. Crooke, M.A. Henderson, S. Sriram, D. Mrelashvili, S. Vosslamber, et al., Using biomarkers to predict progression from clinically isolated syndrome to multiple sclerosis, J. Clin. Bioinf. 3 (2013) 18.
[36] C.F. Spurlock 3rd, G. Shaginurova, J.T. Tossberg, J.D. Hester, N. Chapman, Y. Guo, et al., Profiles of long noncoding RNAs in human naive and memory T cells, J. Immunol. 199 (2017) 547–558.
[37] C.F. Spurlock 3rd, J.T. Tossberg, Y. Guo, S.P. Collier, P.S. Crooke 3rd, T.M. Aune, Expression and functions of long noncoding RNAs during human T helper cell differentiation, Nat. Commun. 6 (2015) 6932.
[38] M. Soutto, W. Zhou, T.M. Aune, Cutting edge: distal regulatory elements are required to achieve selective expression of IFN-gamma in Th1/Tc1 effector cells, J. Immunol. 169 (2002) 6664–6667.
[39] J. Schonborn, J. Oberstrass, E. Breyel, J. Tittgen, J. Schumacher, N. Lukacs, Monoclonal-antibodies to double-stranded-RNA as probes of RNA structure in crude nucleic-acid extracts, Nucleic Acids Res. 19 (1991) 2993–3000.
[40] A.M. Bolger, M. Lohse, B. Usadel, Trimmomatic: a flexible trimmer for Illumina sequence data, Bioinformatics 30 (2014) 2114–2120.
[41] B. Li, C.N. Dewey, RSEM: accurate transcript quantification from RNA-Seq data with or without a reference genome, BMC Bioinf. 12 (2011) 323.
[42] M.D. Robinson, D.J. McCarthy, G.K. Smyth, edgeR: a Bioconductor package for differential expression analysis of digital gene expression data, Bioinformatics 26 (2010) 139–140.
[43] J. Jurka, Repbase Update - a database and an electronic journal of repetitive elements, Trends Genet. 16 (2000) 418–420.
[44] T.M. Aune, P.S. Crooke, A.E. Patrick, J.T. Tossberg, N.J. Olsen, C.F. Spurlock, Expression of long non-coding RNAs in autoimmunity and linkage to enhancer function and autoimmune disease risk genetic variants, J. Autoimmun. 81 (2017) 99–109.
[45] Q.G. Wang, P.L. Jia, Z.M. Zhao, VirusFinder: software for efficient and accurate detection of viruses and their integration sites in host genomes through next generation sequencing data, PLoS One 8 (2013) e64465.
[46] J.T. Robinson, H. Thorvaldsdottir, W. Winckler, M. Guttman, E.S. Lander, G. Getz, et al., Integrative genomics viewer, Nat. Biotechnol. 29 (2011) 24–26.
[47] D. Hnisz, B.J. Abraham, T.I. Lee, A. Lau, V. Saint-Andre, A.A. Sigova, et al., Super-enhancers in the control of cell identity and disease, Cell 155 (2013) 934–947.
[48] W.B. Li, D. Notani, M.G. Rosenfeld, Enhancers as non-coding RNA transcription units: recent insights and future perspectives, Nat. Rev. Genet. 17 (2016) 207–223.
[49] G. Natoli, J.C. Andrau, Noncoding transcription at enhancers: general principles and functional models, Annu. Rev. Genet. 46 (2012) 1–19.
[50] S. Pott, J.D. Lieb, What are super-enhancers? Nat. Genet. 47 (2015) 8–12.
[51] G. Vahedi, Y. Kanno, Y. Furumoto, K. Jiang, S.C.J. Parker, M.R. Erdos, et al., Super-enhancers delineate disease-associated regulatory nodes in T cells, Nature 520 (2015) 558–562.
[52] W.M. Liu, W.M. Chu, P.V. Choudary, C.W. Schmid, Cell stress and translational inhibitors transiently increase the abundance of mammalian Sine transcripts, Nucleic Acids Res. 23 (1995) 1758–1765.
[53] A.J. Stein, G. Fuchs, C.M. Fu, S.L. Wolin, K.M. Reinisch, Structural insights into RNA quality control: the Ro autoantigen binds misfolded RNAs via its central cavity, Cell 121 (2005) 529–539.
[54] S.L. Wolin, T. Cedervall, The LA protein, Annu. Rev. Biochem. 71 (2002) 375–403.
[55] H.T. Porath, B.A. Knisbacher, E. Eisenberg, E.Y. Levanon, Massive A-to-I RNA editing is common across the Metazoa and correlates with dsRNA abundance, Genome Biol. 18 (2017) 185.
[56] V. Tarallo, Y. Hirano, B.D. Gelfand, S. Dridi, N. Kerur, Y. Kim, et al., DICER1 loss and Alu RNA induce age-related macular degeneration via the NLRP3 inflammasome and MyD88, Cell 149 (2012) 847–859.

[57] B. Bonaci-Nikolic, I. Jeremic, S. Andrejevic, M. Sefik-Bukilica, N. Stojsavljevic, J. Drulovic, Anti-double stranded DNA and lupus syndrome induced by interferon-beta therapy in a patient with multiple sclerosis, Lupus 18 (2009) 78–80.
[58] J.C. Crispin, E. Diaz-Jouanen, Systemic lupus erythematosus induced by therapy with interferon-beta in a patient with multiple sclerosis, Lupus 14 (2005) 495–496.
[59] M.W. Nortvedt, T. Riise, K.M. Myhr, H.I. Nyland, B.R. Hanestad, Type I interferons and the quality of life of multiple sclerosis patients. Results from a clinical trial on interferon alfa-2a, Mult. Scler. 5 (1999) 317–322.
[60] C.H. Polman, H.P. Hartung, The treatment of multiple-sclerosis - current and Future, Curr. Opin. Neurol. 8 (1995) 200–209.
[61] D.E. Goodkin, Interferon beta-1b, Lancet 344 (1994) 1702–1703.
[62] K.M. Myhr, T. Riise, F.E. Green Lilleas, T.G. Beiske, E.G. Celius, A. Edland, et al., Interferon-alpha2a reduces MRI disease activity in relapsing-remitting multiple sclerosis. Norwegian Study Group on Interferon-alpha in Multiple Sclerosis, Neurology 52 (1999) 1049–1056.
[63] H.S. Panitch, R.L. Hirsch, J. Schindler, K.P. Johnson, Treatment of Multiple-Sclerosis with Gamma-interferon - exacerbations associated with activation of the immune-system, Neurology 37 (1987) 1097–1102.
[64] G. Arellano, E. Acuna, L.I. Reyes, P.A. Ottum, P. De Sarno, L. Villarroel, et al., Th1 and Th17 cells and associated cytokines discriminate among clinically isolated syndrome and multiple sclerosis phenotypes, Front. Immunol. 8 (2017) 753.
[65] M. Su, D.L. Han, J. Boyd-Kirkup, X.M. Yu, J.D.J. Han, Evolution of Alu elements toward enhancers, Cell Rep. 7 (2014) 376–385.
[66] G. Guarda, M. Braun, F. Staehli, A. Tardivel, C. Mattmann, I. Forster, et al., Type I interferon inhibits interleukin-1 production and inflammasome activation, Immunity 34 (2011) 213–223.
[67] A. Billiau, Anti-inflammatory properties of Type I interferons, Antivir. Res. 71 (2006) 108–116.
[68] A.N. Theofilopoulos, R. Baccala, B. Beutler, D.H. Kono, Type I interferons (alpha/beta) in immunity and autoimmunity, Annu. Rev. Immunol. 23 (2005) 307–336.
[69] T.M. Aune, C.W. Pierce, Activation of a suppressor T-cell pathway by interferon, Proc. Natl. Acad. Sci. U. S. A 79 (1982) 3808–3812.